# A *Drosophila* screen of schizophrenia-related genes highlights the requirement of neural and glial matrix metalloproteinases for neuronal remodeling

Shir Keret[1,2], Hagar Meltzer[1,2*], Neta Marmor-Kollet[1,2,3] Oren Schuldiner[1,2*]

[1] Department of Molecular Cell Biology, Weizmann Institute of Science, Rehovot, Israel

[2] Department of Molecular Neuroscience, Weizmann Institute of Science, Rehovot, Israel

[3] Current affiliation: Department of Biology, Brandeis University, MA, USA

* Correspondence to: hagar.meltzer@weizmann.ac.il; oren.schuldiner@weizmann.ac.il

**Abstract**

Schizophrenia (SCZ) is a multifactorial neuropsychiatric disorder of complex and mostly unknown etiology, affected by genetic, developmental and environmental factors. Neuroanatomical abnormalities, such as loss of grey matter, are apparent prior to the onset of symptoms, suggesting neurodevelopmental origin. Indeed, it has been hypothesized, and recently experimentally supported, that SCZ is associated with dysregulation of developmental synaptic pruning. Here, we explore the molecular link between SCZ-associated genes and developmental neuronal remodeling. We focused on the *Drosophila* mushroom body (MB), which undergoes stereotypic remodeling during metamorphosis. We conducted a loss-of-function screen in which we knocked down, in either glia or neurons, *Drosophila* homologs of human genes that are associated with SCZ based on genomic studies (GWAS). Out of our 'positive hits', we focused on matrix metalloproteinases (MMPs), mostly known for their role in remodeling of the extracellular matrix. Our combinatorial loss-of-function experiments suggest that *Drosophila* MMPs, which are closely related to mammalian MMPs, are required in neurons and in glia for the pruning of MB axons. Our results shed new light on potential molecular players underlying neurodevelopmental defects in SCZ and highlight the advantage of genetically tractable model organisms in the study of human neurodevelopmental disorders.

## Introduction

Following its initial establishment, the developing nervous system of both vertebrates and invertebrates undergoes remodeling to shape its mature connectivity. In humans, developmental neuronal remodeling occurs postnatally and includes degenerative events such as retraction of synapses and large-scale axon elimination. While these processes occur most prominently during the first two years of life, they continue until after adolescence (Luo & O'Leary, 2005; Schuldiner & Yaron, 2015). Defects in neuronal remodeling have long been hypothesized to be one of the underlying causes of neuropsychiatric disorders, including schizophrenia (SCZ; Feinberg, 1982; Penzes et al., 2011).

SCZ is a severe, multifactorial mental health condition affecting ~1% of the population. It is characterized by delusions, hallucinations, social withdrawal and cognitive deficits, typically onsetting during the late teens to early adulthood (McCutcheon et al., 2020). It is known from MRI studies that structural abnormalities in the brain, such as reduction in gray matter and ventricular enlargement, may precede the onset of psychotic symptoms, implying neurodevelopmental origin (Brent et al., 2013; Omlor et al., 2025; Suzuki et al., 2002; Zikidi et al., 2020). It has been suggested, for many years, that the characteristic neuroanatomical alterations in individuals with SCZ are due to dysregulation of neuronal remodeling, specifically over-pruning of synapses (Feinberg, 1982; Hoffman & Dobscha, 1989; Huttenlocher & Dabholkar, 1997; Keshavan et al., 1994; Peter R, 1979). The first experimental evidence to support this hypothesis came several years ago, and associated SCZ with excessive expression of complement components leading to increased synapse elimination by microglia (Sekar et al., 2016). This work as well as others highlighted glia, including microglia and astrocytes, as key mediators of synapse pruning in normal development as well as in SCZ and other neuropathologies (Reviewed in Laricchiuta et al., 2024; Notter, 2021; Scott-Hewitt et al., 2023). Still, the molecular basis of SCZ risk and its link to abnormalities in neuronal remodeling remains mostly unknown.

*Drosophila melanogaster* is an ideal model to study neuronal remodeling, due to its unparalleled genetic toolkit combined with its massive stereotypic circuit remodeling during metamorphosis (Truman, 1990; Yaniv & Schuldiner, 2016). Our focus is on the

64 *Drosophila* mushroom body (MB), a brain structure that functions as a center of olfactory
65 learning and memory (Heisenberg, 1998). The MB is comprised of three types of intrinsic
66 neurons, known as Kenyon cells (KCs), which are sequentially born from identical
67 neuroblasts (Fig. 1A). Out of the three KC types (γ, α'/β' and α/β), only the first-born γ-
68 KCs undergo stereotypic remodeling. When they initially grow, in the embryonic and early
69 larval stages, γ-KCs project axons that bifurcate to form vertical and medial lobes. At the
70 early pupal stage (~6-18 hours after puparium formation; h APF) both axonal lobes prune
71 up to their branchpoint. Subsequently, γ-KCs initiate axon regrowth to create the adult-
72 specific medially projecting γ-lobe (Lee et al., 1999; Yaniv & Schuldiner, 2016; Fig. 1A).
73 Importantly, glia were shown, by our lab and others, to actively participate in the
74 remodeling of γ-KCs (Awasaki et al., 2011; Awasaki & Ito, 2004; Boulanger et al., 2021;
75 Hakim et al., 2014; Marmor-Kollet et al., 2023; Watts et al., 2004). Three glial subtypes
76 are present around the MB: cortex glia, ensheathing glia and astrocyte-like glia (hereafter
77 referred to as astrocytes; Freeman, 2015). Astrocytes are the main scavengers of axonal
78 debris following pruning (Hakim et al., 2014; Tasdemir-Yilmaz & Freeman, 2014).
79 Additionally, inhibiting astrocytic functions results in brain-wide defects in synapse
80 elimination (Tasdemir-Yilmaz & Freeman, 2014). Moreover, we recently demonstrated
81 that astrocytes actively infiltrate the axon bundle prior to pruning to facilitate axon
82 defasciculation and elimination (Marmor-Kollet et al., 2023).
83 *Drosophila* is routinely used to study human neurodegenerative and neuropsychiatric
84 disorders (Lessing & Bonini, 2009; van Alphen & van Swinderen, 2013), and SCZ-
85 associated genes were shown to affect MB structure, activity and function in memory and
86 sleep (Furukubo-Tokunaga, 2009; Hidalgo et al., 2021; Sawamura et al., 2008). Here, we
87 harness the fly genetic toolkit and the well-characterized remodeling of the MB to delve
88 into the molecular underpinnings of the long-standing hypothesis that defects in neuronal
89 remodeling contribute to SCZ etiology. We systematically examine how MB remodeling
90 is affected by perturbations in *Drosophila* genes whose human homologs have been
91 associated with SCZ. Our findings identify novel players in axon pruning and further
92 highlight the significance of glial contribution to remodeling, providing a solid basis for
93 future research on the neurodevelopmental molecular origin of SCZ.

## Results

### *Drosophila homologs of human SCZ-associated genes are dynamically expressed in developing mushroom body γ-KCs and in astrocytes*

We searched genome-wide association studies (GWAS) for candidate genes that have single nucleotide polymorphism (SNPs) in SCZ patients (339 genes; Hamshere et al., 2013; Wu et al., 2017; szdb.org/index.html), which is a compilation of data from the Psychiatric Genomics Consortium (PGC) and CLOZUK. We converted the SNP-containing genes to their *Drosophila* homologs using HumanMine (Lyne et al., 2022), resulting in 252 genes (Fig. 1B; Supplementary excel file 1). To narrow our candidate list to genes that are potentially required for MB pruning, we first used our previously generated transcriptional atlas of developing γ-KCs (Alyagor et al., 2018) to identify 196 genes that are expressed above threshold levels, out of which 82 showed dynamic expression (Fig. S1). Next, we narrowed our list to genes that are specifically upregulated during or prior to γ-axon pruning (Fig. 1B, Fig. 1C clusters III-VI highlighted). This process resulted in 32 candidate genes, out of which 29 had available RNA-interference (RNAi) fly lines for loss-of-function (LOF) screening (Fig.1B; Supplementary excel file 1). Due to the known significance of glia in pruning, in parallel we also examined a second transcriptional dataset, of larval and adult astrocytes, previously generated in the lab (Marmor-Kollet et al., 2023). Out of the 252 *Drosophila* homologs of SCZ-associated genes, 173 are expressed in astrocytes above threshold levels (Fig.1B; Supplementary excel file 1). Out of these, 8 are upregulated in late larval (3$^{rd}$ instar larvae; L3) compared to adult astrocytes (Fig. 1D; Supplementary excel file 1), suggesting a potential role in axon pruning. All 8 genes had available RNAi lines for screening.

### *Drosophila homologs of human SCZ-associated genes are required in neurons and glia for γ-axon pruning*

We screened candidate genes using a LOF strategy by tissue-specific expression of RNAi-species via the Gal4-UAS system (Brand & Perrimon, 1993). For KD in γ-KCs, we used the pan-KC driver OK107-Gal4, which is strongly expressed in all KC types (α/β, α'/β' and γ), combined with a second, independent binary system (Riabinina & Potter, 2016) to specifically visualize γ-KCs in the adult MB (R71G10-QF2 driving mtdT-HA; Fig. 2A). Notably, although remodeling of MB γ-KCs occurs during metamorphosis, unpruned

125 larval axons persist until adulthood. Thus, adult MBs reflect abnormalities that occurred
126 during development. Out of the 29 genes we screened, OK107-Gal4-driven KD of 4 genes
127 resulted in lethality, 11 genes displayed varying degrees of pruning defects ('positive hits';
128 Fig. 2B-N), and one gene led to abnormal MB morphology (Fig. S2). In parallel, we used
129 a similar strategy to screen the 8 candidate genes in glia - by driving RNAi using the
130 strong pan-glial driver Repo-Gal4, combined with R71G10-QF2-driven mtdT to visualize
131 γ-KCs (Fig. 2O). Strikingly, KD of 7 of the 8 genes resulted in γ-axon pruning defects (Fig.
132 2P-X).

133 ***Drosophila MMPs are required in KCs and glia for γ axon pruning***

134 Many of the 'positive hits' in the screen are promising directions for further exploration.
135 Interestingly, two genes - Syntaxin13 (Syx13) and Matrix Metalloproteinase 2 (Mmp2) -
136 emerged as required for pruning in both neurons and glia. We decided to delve deeper
137 into Mmp2, as a previous, CRISPR-based screen done by our lab also found it to be
138 required in γ-KCs for axon pruning (Meltzer et al., 2019).
139 MMPs are extracellular proteases that cleave extracellular matrix (ECM) components
140 (Page-McCaw et al., 2007; Sreesada et al., 2025). In the mouse there are 23 MMPs,
141 while the zebrafish genome encodes 25 MMPs. The *Drosophila* genome, in contrast,
142 encodes only two MMPs – Mmp1 and Mmp2 – which together have 13 predicted isoforms,
143 most of which are likely secreted, while each Mmp also has a glycosylphosphatidylinositol
144 (GPI)-anchored isoform (LaFever et al., 2017). The significantly reduced complexity
145 makes *Drosophila* MMPs an ideal model system to uncover novel insights into their roles
146 in neuronal remodeling. Our transcriptional datasets indicate that both MMPs are
147 dynamically expressed in γ-KCs, as well as in larval astrocytes (Fig. 3A). We thus decided
148 to KD Mmp1 in both KCs and glia, and compare it to Mmp2 (Fig. 3B-I). Blinded ranking
149 by two independent investigators (Fig. S3) established that the pruning defect induced by
150 KD of Mmp1 or Mmp2 is significant compared to controls in glia (Fig. 3B-E). KD of Mmp1
151 in KCs results in a mild pruning defect, not reaching statistical significance, while
152 knockdown of Mmp2 is significant compared to controls (Fig. 3F-I). Importantly, we
153 validated the efficiency of the Mmp1 RNAi line in reducing protein levels using an Mmp1
154 antibody (Fig. S4). The specific Mmp2 RNAi line that we used was previously
155 demonstrated to efficiently reduce Mmp2 protein levels (Harmansa et al., 2023).

156 We next used CRISPR/Cas9 to generate a novel, predicted null *mmp2* mutant allele. Due
157 to its (expected) lethality, we employed MARCM (Lee & Luo, 1999) to generate
158 homozygous mutant γ-KC clones. However, *mmp2*$^{\Delta 54\text{-}120.PC}$ clones did not present
159 pruning defects (Fig. S5), consistent with its predicted function as a predominantly
160 secreted protein, and therefore a non-cell autonomous role. Thus, to further validate our
161 findings, we tested a second RNAi line targeting Mmp2, which similarly showed pruning
162 defects when driven in glia (Fig. 3L), and a very mild defect in KCs (Fig. S6C).
163 To further explore the requirement of Mmp1, we tested a dominant negative (DN) variant
164 previously generated by the Page-McCaw lab (Glasheen et al., 2009). When expressed
165 in glia, Mmp1-DN resulted in a severe γ-axon pruning defect (Fig. 3K), while expressing
166 it in KCs results in a mild pruning defect (Fig. S6B), reinforcing the reduced requirement
167 of Mmp1 in γ-KCs compared to glia.
168 Notably, the initial growth of γ-KC axons, as evident at the onset of pupariation, is
169 unaffected by KD of either Mmp1 or Mmp2, in neither KCs nor glia (Fig. S7), highlighting
170 their specific role in the axon remodeling phase.
171 Taken together, our data suggests that while both MMPs are required in glia and in KCs
172 for γ-axon remodeling.

173 ***Analysis of combinatorial MMP knockdown in both KCs and glia***

174 Since most Mmp1 and Mmp2 isoforms are secreted, we speculated that both are secreted
175 in parallel from KCs and glia to promote axon pruning. Therefore, we preformed different
176 single and double KD combinations of Mmp1 and/or Mmp2 in KCs and/or glia (Fig. 4).
177 Our data and quantification (by two independent investigators, see Methods and Fig. S3)
178 draw two main conclusions: first, while both Mmp1 and Mmp2 are required for pruning,
179 using the available drivers and RNAi reagents, the observed phenotypes of Mmp2 KD
180 are more severe in all conditions. Second, while Mmp1/2 expression from both KCs and
181 glia is required for pruning of γ-axons, the main source is likely glia, as KD of a single or
182 double MMP in both glia and neurons did not further exacerbate the pruning defect
183 severity compared to the respective KD in glia only (Fig. 4, quantified in M-O).
184 Due to the major glial contribution, combine with the known astrocytic involvement in
185 remodeling and the expression data (Fig. 3A), we decided to also test KD using the
186 astrocyte-specific driver alrm-Gal4, which indeed resulted in mild pruning defect in the

case of Mmp2 (Fig. S8). The mild phenotype can be explained by weaker Gal4 expression compared to Repo-Gal4, or due to involvement of additional glial subtypes. Unfortunately, our attempts to analyze other glial subtypes were abruptly terminated (see acknowledgements).

Taken together, our results suggest that while both MMPs affect pruning likely via secretion from both neurons and glia, the strongest requirement for MB γ axon pruning comes from MMPs secretion by glia - at least partially by astrocytes.

## Discussion

Four decades ago, Feinberg hypothesized that SCZ is caused by aberrant synaptic pruning during adolescence: “too many, too few or the wrong synapses are eliminated” (Feinberg, 1982). In recent years, accumulating findings are providing experimental support of this hypothesis (Keshavan et al., 2020; Sekar et al., 2016; Sellgren et al., 2019). In this work, we aimed to further explore the molecular association of SCZ-related genes with defective neuronal remodeling, by utilizing the stereotypic remodeling of the *Drosophila* MB.

In a genetic LOF screen for *Drosophila* homologs of human genes that contain SNPs associated with SCZ, about 40% of the genes we screened within the neurons (11 out of 29) were found to have a role in γ-axon pruning. Additionally, 7 out of 8 genes we screened within the glia were found to have a role in γ-axon pruning. This high rate of ‘positive hits’ strengthens the link between SCZ-associated genes and defects in developmental neuronal remodeling and emphasizes glia’s major role. Notably, we focused on genes that are upregulated prior to pruning, but future efforts to overexpress genes that are downregulated prior to pruning might also reveal interesting insights.

While many of the ‘positive hits’ are fascinating candidates for further research, in this study we decided to focus on the role of MMPs in neuronal remodeling, for several reasons. First, Mmp2 was found to be required in both glia and neurons for γ-axon pruning. This is of particular interest due to the speculated role of glia in abnormal synaptic pruning in SCZ patients. Second, previous reports have highlighted the link between MMPs and the pathophysiology of SCZ. Specifically, elevated levels of MMPs, most prominently Mmp9, were shown to correlate with SCZ risk and cognitive impairment

218 (Dickerson et al., 2023; Kudo et al., 2020; Schoretsanitis et al., 2021; Seitz-Holland et al.,
219 2022). While it has been suggested that this correlation is via MMP-dependent changes
220 in dendritic spine morphology (Lepeta et al., 2017), the precise mechanism remains
221 poorly understood. Of note, the *Drosophila* MMPs are evolutionary conserved (LaFever
222 et al., 2017; Llano et al., 2002), highlighting their potential relevance and providing a
223 simplified and powerful model system for mechanistic exploration.
224 MMPs are known for their roles in tissue remodeling by cleaving substrates in the ECM
225 (Page-McCaw et al., 2007), and are well studied in the cancer field (Cox, 2021; Overall &
226 López-Otín, 2002), but their mechanistic function in the developing nervous system is
227 less characterized (e.g., Broadie et al., 2011; Dear et al., 2016; Gore et al., 2021). MMPs
228 are known to be secreted by neurons and glia, and are thought to facilitate synaptic
229 remodeling of dendritic spines (Huntley, 2012). In adult rodent brains, pharmacologically-
230 (Szklarczyk et al., 2002) or injury- (Pijet et al., 2019) induced dendritic remodeling is
231 suggested to occur via Mmp9. In the developmental remodeling of *Drosophila* dendritic
232 arborization (da) neurons, both Mmp1 and Mmp2 were shown to be required for the
233 elimination of severed dendritic branches in a non-cell autonomous manner (Kuo et al.,
234 2005). Their source, as well as the mechanism by which they promote dendrite removal,
235 remain unknown (the authors speculate they are secreted from phagocytic cells – at the
236 time they suggested blood cells, but given more recent studies from the same lab,
237 epidermal cells are more likely; Han et al., 2014). Interestingly, MMPs were also shown
238 to mediate dendrite reshaping of da neurons in the mature fly via local degeneration of
239 the basement membrane, further reinforcing their significance in refining the mature
240 nervous system (Yasunaga et al., 2010). Finally, it was shown that Mmp1 is upregulated
241 in astrocytes after traumatic brain injury (Li et al., 2024), and in ensheathing glia following
242 ventral nerve cord injury to promote axonal debris clearance (Purice et al., 2017).
243 The mechanism by which MMPs promote remodeling of MB γ-axons, and specifically
244 their substrates in this context, remain to be uncovered. Since the main known role of
245 MMPs is cleaving ECM substrates, they may act as 'path cleaners' for the migration of
246 cells and molecules (Page-McCaw et al., 2007). This function can be relevant to axon
247 pruning in several, non-mutually exclusive ways. One option is that MMPs allow the
248 migration of Myoglianin (Myo), a *Drosophila* TGF-β, in the ECM. Myo is part of the pruning

249 initiation cascade and was shown to be secreted by cortex glia and astrocytes (Awasaki
250 et al., 2011) to eventually promote expression of ecdysone receptor (EcR)-B1, a key
251 regulator of remodeling (Yu et al., 2013; Zheng et al., 2003). Moreover, it was shown that
252 the human Mmp9 can proteolytically activate latent TGF-β (Yu & Stamenkovic, 2000).
253 However, we found that the expression of EcR-B1 in γ-KCs in unaffected by glia or
254 neuronal KD of Mmp1/Mmp2 (Fig. S9). Another option is that MMPs facilitate astrocyte
255 infiltration into the γ-axon bundle at the onset of pruning, that was shown to be required
256 for defasciculation (Marmor-Kollet et al., 2023), and subsequent engulfment of the axonal
257 debris (Hakim et al., 2014; Tasdemir-Yilmaz & Freeman, 2014). Unfortunately, testing this
258 hypothesis requires three binary systems and is beyond the scope of this study. MMPs
259 were also shown to degrade adhesion molecules (Page-McCaw et al., 2007), and our lab
260 previously showed that the adhesion molecule Fasciclin II (FasII) must be downregulated
261 for pruning to occur properly (Bornstein et al., 2015). It is thus possible that MMPs cleave
262 FasII, or other adhesion molecules, to promote axon pruning. Since most *Drosophila*
263 MMP isoforms are secreted (LaFever et al., 2017), together with the finding that they are
264 required from both neuronal and glial origin, it is possible that MMPs are also secreted
265 from additional cells within or around the MB circuit. All the above-mentioned options are
266 promising directions for future research, in hopes of uncovering the mechanisms by which
267 MMPs promote neuronal remodeling.
268 Notably, the main hypothesis in the literature is that SCZ is associated with increased
269 synapse pruning, while in our study KD of SCZ-associated genes resulted in inhibition of
270 pruning, which may seem counter-intuitive at first. However, SNPs can result in loss- but
271 also gain-of-function, which could account for this apparent conflict. In fact, it was
272 previously shown that the SCZ-associated SNP in Mmp9 is in the 3' UTR, and affects
273 Mmp9 mRNA folding which eventually results in higher Mmp9 compared to WT (Lepeta
274 et al., 2017).
275 We recognize that the current study explores pruning of long stretches of axons, while
276 SCZ is mainly associated with defective synapse pruning. More generally, flies could
277 never model the complexities associated with human psychiatric conditions, nor directly
278 offer therapeutic targets. Nonetheless, this simple and genetically accessible model
279 enables us to uncover conserved neurodevelopmental principles and concepts.

280 Understating the neurodevelopmental role of MMPs may provide insights into brain ECM
281 dynamics throughout development, and specifically during neuronal remodeling.

282 **Materials and methods**

283 *Gene selection for the screen*
284 Human genes that contain SNPs associated with SCZ were collected from two studies:
285 PGC2 & CLOZUK (Wu et al., 2017; Supplemental excel file 1). These genes were
286 converted to their *Drosophila melanogaster* homologs using HumanMine (Supplemental
287 excel file 1). In cases of multiple fly homologs for a single human gene, we decided to
288 include all of them.

289 *Drosophila melanogaster rearing and strains*
290 All fly strains were reared under standard laboratory conditions at 25°C on molasses-
291 containing food. Males and females were chosen at random. Unless specifically stated
292 otherwise, the relevant developmental stage is adult, which refers to 3-5 days post
293 eclosion. The RNA lines used for the screen are detailed in Table 1. The following lines
294 were obtained for the Bloomington Drosophila Stock Center (BDSC): Luciferase RNAi
295 (used as control for RNAi experiments; #31603), CG2712 RNAi (used as control for RNAi
296 experiments; #57418), Mmp1 RNAi (#31489), Alrm-Gal4 (#67032), Repo-Gal4 (#7415),
297 OK107-Gal4 (#854), TIFR-Gal4 (#90392), QUAS-mtdTomato-3xHA (#30004), Mmp2-
298 gRNA (#82521). R71G10-QF2 was previously generated by our lab (Bornstein et al.,
299 2021). R71G10-Gal4 on the 2$^{nd}$ chromosome was previously generated by our lab
300 (Alyagor et al., 2018)A second Mmp2 RNAi line was obtained from the Vienna Drosophila
301 Resource Center (VDRC; #107888). Line UAS-Mmp1.f1$^{\Delta Cat1}$ was a generous gift from
302 Andrea Page-McCaw. See full genotypes (ordered by specific figure panels) in Table 2.
303

304

| Gene | TRiP # | BDSC # | Phenotype |
|---|---|---|---|
| **KC screen** | | | |
| tartan | HM05011 | 28525 | WT-like |
| Fish-lips | HM05054 | 28568 | WT-like |
| retinal degeneration A | JF03371 | 29435 | WT-like |
| Ppr-Y | HMS00819 | 33882 | WT-like |
| FER tyrosine kinase | HMS00249 | 33375 | WT-like |
| Matrix metalloproteinase 2 | HMJ23143 | 61309 | Pruning defect |
| Phospholipase C at 21C | HMS00436 | 32438 | Pruning defect |
| Proteasome alpha3 subunit | HMS05889 | 77145 | Lethal |
| Regulatory particle non-ATPase 7 | HMS00096 | 34787 | Lethal |
| Syntaxin 13 | HMS01723 | 38525 | Pruning defect |
| anterior pharynx defective 1 | HMS01693 | 38249 | Lethal |
| BNIP3 | HMJ02058 | 42494 | Pruning defect |
| liquid facets | HMJ22079 | 58130 | Mild pruning defect |
| eukaryotic translation release factor 1 | HMS05812 | 67900 | Abnormal MB |
| DIP-kappa | HM04050 | 31740 | WT-like |
| MYPT-75D | HMS01166 | 34688 | WT-like |
| Protein phosphatase 19C | HMS01841 | 38372 | Pruning defect |
| GTPase activating protein and centrosome-associated | HMS01132 | 34976 | WT-like |
| Ran-binding protein M | HMC05142 | 61172 | Pruning defect |
| Na[+]-driven anion exchanger 1 | HMC05184 | 62177 | WT-like |
| minidiscs | HMC05214 | 62207 | WT-like |
| Serine-arginine protein kinase at 79D | HMC04154 | 55881 | WT-like |
| Ypel | HM05209 | 29530 | Pruning defect |
| Akt1 | HMS00007 | 33615 | Lethal |
| absent, small, or homeotic discs 2 | HMC05816 | 64942 | Mild pruning defect |
| Fmr1 | HMS00248 | 34944 | WT-like |
| Arginine methyltransferase 1 | GL01072 | 36891 | WT-like |
| Ge-1 | HMS00340 | 32349 | Pruning defect |
| crooked legs | HMS02202 | 41669 | Pruning defect |
| **Pan-glial screen** | | | |
| ballchen | HMC04017 | 55330 | Pruning defect |
| Lachesin | HMS01756 | 38536 | Pruning defect |
| Syntaxin 13 | HMS01723 | 38536 | Pruning defect |
| Arginine methyltransferase 1 | JF01306 | 31348 | Pruning defect |
| Nucleostemin 1 | HMJ23534 | 61950 | Lethal |
| Matrix metalloproteinase 2 | HMJ23143 | 61309 | Pruning defect |
| Kinesin light chain | HMS02429 | 42597 | Pruning defect |
| Swiprosin-1 | JF01160 | 31585 | Pruning defect |

305 **Table 1.** RNAi lines used in the KC screen (using OK107-Gal4) and the pan-glial screen (using
306 Repo-Gal4) and their KD phenotypes.

| Figure panel | Full genotype | Comment |
|---|---|---|
| 2C | $y^1$ $v^1$/+ or Y; R71G10-QF2, QUAS-mtdT:3xHA/+; P{y[+t7.7] v[+t1.8]=TRiP.JF01355}attP2/+; OK107-Gal4/+ | UAS-Luciferase-RNAi (BL#31603) |
| 2D | $y^1$ $v^1$/+ or Y; R71G10-QF2, QUAS-mtdT:3xHA/P{y[+t7.7] v[+t1.8]=TRiP.HMJ23143}attP40;; OK107-Gal4/+ | UAS-Mmp2-RNAi (BL#61309) |
| 2E | $y^1$ sc* $v^1$ $sev^{21}$/+ or Y; R71G10-QF2, QUAS-mtdT:3xHA/+; P{y[+t7.7] v[+t1.8]=TRiP.HMS00436}attP2/+; OK107-Gal4/+ | UAS-Plc21c-RNAi (BL#32438) |
| 2F | $y^1$ sc* $v^1$ $sev^{21}$/+ or Y; R71G10-QF2, QUAS-mtdT:3xHA/P{y[+t7.7] v[+t1.8]=TRiP.HMS01723}attP40;; OK107-Gal4/+ | UAS-Syx13-RNAi (BL#38525) |
| 2G | $y^1$ sc* $v^1$ $sev^{21}$/+ or Y; R71G10-QF2, QUAS-mtdT:3xHA/+; P{y[+t7.7] v[+t1.8]=TRiP.HMS01841}attP2/+; OK107-Gal4/+ | UAS-Pp4-19C-RNAi (BL#38372) |
| 2H | $y^1$ sc* $v^1$ $sev^{21}$/+ or Y; R71G10-QF2, QUAS-mtdT:3xHA/P{y[+t7.7] v[+t1.8]=TRiP.HMC05142}attP40;; OK107-Gal4/+ | UAS-RanBPM-RNAi (BL#61172) |
| 2I | $y^1$ $v^1$/+ or Y; R71G10-QF2, QUAS-mtdT:3xHA/+; P{y[+t7.7] v[+t1.8]=TRiP.HM05209}attP2/+; OK107-Gal4/+ | UAS-Ypel-RNAi (BL#29530) |
| 2J | $y^1$ sc* $v^1$ $sev^{21}$/+ or Y; R71G10-QF2, QUAS-mtdT:3xHA/+; P{y[+t7.7] v[+t1.8]=TRiP.HMS00340}attP2/+; OK107-Gal4/+ | UAS-Ge-1-RNAi (BL#32349) |
| 2K | $y^1$ $v^1$ /+ or Y; R71G10-QF2, QUAS-mtdT:3xHA/P{y[+t7.7] v[+t1.8]=TRiP.HMS02202}attP40;; OK107-Gal4/+ | UAS-crol-RNAi (BL#41669) |
| 2L | $y^1$ $v^1$ /+ or Y; R71G10-QF2, QUAS-mtdT:3xHA/P{y[+t7.7] v[+t1.8]=TRiP.HMJ02058}attP40;; OK107-Gal4/+ | UAS-BNIP3-RNAi (BL#42494) |
| 2M | $y^1$ $v^1$ /+ or Y; R71G10-QF2, QUAS-mtdT:3xHA/P{y[+t7.7] v[+t1.8]=TRiP.HMJ22079}attP40;; OK107-Gal4/+ | UAS-lqf-RNAi (BL#58130) |
| 2N | $y^1$ sc* $v^1$ $sev^{21}$/+ or Y; R71G10-QF2, QUAS-mtdT:3xHA/P{y[+t7.7] v[+t1.8]=TRiP.HMC05816}attP40;; OK107-Gal4/+ | UAS-ash2-RNAi (BL#64942) |
| 2Q | $y^1$ sc* $v^1$ $sev^{21}$/+ or Y; R71G10-QF2, QUAS-mtdT:3xHA/ P{y[+t7.7] v[+t1.8]=TRiP.HMC04724}attP40; Repo-Gal4 UAS-CD8::GFP/+ | UAS-CG2712-RNAi (BL#57418) |
| 2R | $y^1$ $v^1$/+ or Y; R71G10-QF2, QUAS-mtdT:3xHA/P{y[+t7.7] v[+t1.8]=TRiP.HMJ23143}attP40; Repo-Gal4 UAS-CD8::GFP/+ | UAS-Mmp2-RNAi (BL#61309) |
| 2S | $y^1$ $v^1$/+ or Y; R71G10-QF2, QUAS-mtdT:3xHA/P{y[+t7.7] v[+t1.8]=TRiP.HMC04017}attP40; Repo-Gal4 UAS-CD8::GFP/+ | UAS-ball-RNAi (BL#55330) |
| 2T | $y^1$ sc* $v^1$ $sev^{21}$/+ or Y; R71G10-QF2, QUAS-mtdT:3xHA/P{y[+t7.7] v[+t1.8]=TRiP.HMS01723}attP40; Repo-Gal4 UAS-CD8::GFP/+ | UAS-Syx13-RNAi (BL#38525) |
| 2U | $y^1$ sc* $v^1$ $sev^{21}$/+ or Y; R71G10-QF2, QUAS-mtdT:3xHA/P{y[+t7.7] v[+t1.8]=TRiP.HMS01756}attP40; Repo-Gal4 UAS-CD8::GFP/+ | UAS-Lac-RNAi (BL#38536) |
| 2V | $y^1$ $v^1$/+ or Y; R71G10-QF2, QUAS-mtdT:3xHA/+; P{y[+t7.7] v[+t1.8]=TRiP.JF01306}attP2/Repo-Gal4 UAS-CD8::GFP | UAS-Art1-RNAi (BL#31348) |
| 2W | $y^1$ $v^1$/+ or Y; R71G10-QF2, QUAS-mtdT:3xHA/+; P{y[+t7.7] v[+t1.8]=TRiP.JF01160}attP2/Repo-Gal4 UAS-CD8::GFP | UAS-Swip-1-RNAi (BL#31585) |
| 2X | $y^1$ sc* $v^1$ $sev^{21}$/+ or Y; R71G10-QF2, QUAS-mtdT:3xHA/P{y[+t7.7] v[+t1.8]=TRiP.HMS02429}attP40; Repo-Gal4 UAS-CD8::GFP/+ | UAS-Klc-RNAi (BL#42597) |
| S2A | $y^1$ $v^1$/+ or Y; R71G10-QF2, QUAS-mtdT:3xHA/+; P{y[+t7.7] v[+t1.8]=TRiP.JF01355}attP2/+; OK107-Gal4/+ | UAS-Luciferase-RNAi (BL#31603) |
| S2B | $y^1$ $v^1$ /+ or Y; R71G10-QF2, QUAS-mtdT:3xHA/P P{y[+t7.7] v[+t1.8]=TRiP.HMS05812}attP40;; OK107-Gal4/+ | UAS-eRF1-RNAi (BL#67900) |
| 3B | $y^1$ sc* $v^1$ $sev^{21}$/+ or Y; R71G10-QF2, QUAS-mtdT:3xHA/ P{y[+t7.7] v[+t1.8]=TRiP.HMC04724}attP40; Repo-Gal4 UAS-CD8::GFP/+ | UAS-CG2712-RNAi (BL#57418) |
| 3C | $y^1$ $v^1$/+ or Y; R71G10-QF2, QUAS-mtdT:3xHA/+; P{y[+t7.7] v[+t1.8]=TRiP.JF01336}attP2/Repo-Gal4, UAS-CD8:GFP | UAS-Mmp1-RNAi (BL#31489) |

| | | |
|---|---|---|
| 3D | $y^1$ $v^1$/+ or Y; R71G10-QF2, QUAS-mtdT:3xHA/P{y[+t7.7] v[+t1.8]=TRiP.HMJ23143}attP40; Repo-Gal4, UAS-CD8:GFP/+ | UAS-Mmp2-RNAi (BL#61309) |
| 3F | $y^1$ $v^1$/+ or Y; R71G10-QF2, QUAS-mtdT:3xHA/+; P{y[+t7.7] v[+t1.8]=TRiP.JF01355}attP2/+; OK107-Gal4/+ | UAS-Luciferase-RNAi (BL#31603) |
| 3G | $y^1$ $v^1$/+ or Y; R71G10-QF2, QUAS-mtdT:3xHA/+; P{y[+t7.7] v[+t1.8]=TRiP.JF01336}attP2/+; OK107-Gal4/+ | UAS-Mmp1-RNAi (BL#31489) |
| 3H | $y^1$ $v^1$/+ or Y; R71G10-QF2, QUAS-mtdT:3xHA/P{y[+t7.7] v[+t1.8]=TRiP.HMJ23143}attP40;; OK107-Gal4/+ | UAS-Mmp2-RNAi (BL#61309) |
| 3J | $y^1$ sc* $v^1$ $sev^{21}$/+ or Y; R71G10-QF2, QUAS-mtdT:3xHA/ P{y[+t7.7] v[+t1.8]=TRiP.HMC04724}attP40; Repo-Gal4 UAS-CD8::GFP/+ | UAS-CG2712-RNAi (BL#57418) |
| 3K | w/+ or Y; R71G10-QF2, QUAS-mtdT:3xHA/+; {UAS-Mmp1.f1$^{\Delta cat}$}1/Repo-Gal4, UAS-CD8:GFP | APM 1044 (Andrea Page-McCaw) |
| 3L | +/+ or Y; R71G10-QF2, QUAS-mtdT:3xHA/UAS-Mmp2-RNAi; Repo-Gal4, UAS-CD8:GFP/+ | UAS-Mmp2-RNAi (VDRC#107888) |
| S3A | R71G10-QF2, QUAS-mtdT:3xHA/+; Repo-Gal4, UAS-CD8:GFP/+ | Canton S (BL#64349) |
| S3B | $y^1$ $v^1$/+ or Y; R71G10-QF2, QUAS-mtdT:3xHA/P{y[+t7.7] v[+t1.8]=TRiP.HMJ23143}attP40;; OK107-Gal4/+ | UAS-Mmp2-RNAi (BL#61309) |
| S3C | $y^1$ $v^1$/+ or Y; R71G10-QF2, QUAS-mtdT:3xHA/P{y[+t7.7] v[+t1.8]=TRiP.HMJ23143}attP40;; OK107-Gal4/+ | UAS-Mmp2-RNAi (BL#61309) |
| S3D | $y^1$ $v^1$/+ or Y; R71G10-QF2, QUAS-mtdT:3xHA/P{y[+t7.7] v[+t1.8]=TRiP.HMJ23143}attP40;; OK107-Gal4/+ | UAS-Mmp2-RNAi (BL#61309) |
| S3E | $y^1$ $v^1$/+ or Y; R71G10-QF2, QUAS-mtdT:3xHA/P{y[+t7.7] v[+t1.8]=TRiP.HMJ23143}attP40; Repo-Gal4, UAS-CD8:GFP/+ | UAS-Mmp2-RNAi (BL#61309) |
| S4A-B | w/$y^1$ $w^{118}$ or Y; R71G10-QF2, QUAS-mtdT:3xHA/+; 57C10-Gal4/+ | $y^1$ ,$w^{118}$ (BL#6598) |
| S4C | w/$y^1$ $w^{118}$ or Y; UAS-mCD4:GFP/+; TIFR-Gal4/+ | TIFR-Gal4 (BL#90392) |
| S4D | w/$y^1$ $w^{118}$ or Y; UAS-mCD4:GFP/+; TIFR-Gal4/P{y[+t7.7] v[+t1.8]=TRiP.JF01336}attP2 | UAS-Mmp1-RNAi (BL#31489) |
| S5B | y,w,hsFlp122, UAS-CD8::GFP/y,w or Y; R71G10-Gal4,G13,Gal80/40A,G13,cn,bw | G13 and 40A are FRTs on 2R and 3R, respectively |
| S5C | y,w,hsFlp122, UAS-CD8::GFP/y,w or Y; R71G10-Gal4,G13,Gal80/40A,G13,*mmp2*$^{\Delta 54\text{-}120.C}$,cn,bw | G13 and 40A are FRTs on 2R and 3R, respectively |
| S6A | $y^1$ $v^1$/+ or Y; R71G10-QF2, QUAS-mtdT:3xHA/+; P{y[+t7.7] v[+t1.8]=TRiP.JF01355}attP2/+; OK107-Gal4/+ | UAS-Luciferase-RNAi (BL#31603) |
| S6B | $y^1$ $v^1$/+ or Y; R71G10-QF2, QUAS-mtdT:3xHA/+; {UAS-Mmp1.f1$^{\Delta cat}$}1/+; OK107-Gal4/+ | APM 1044 (Andrea Page-McCaw) |
| S6C | $y^1$ $v^1$/+ or Y; R71G10-QF2, QUAS-mtdT:3xHA/ UAS-Mmp2-RNAi;; OK107-Gal4/+ | UAS-Mmp2-RNAi (VDRC#107888) |
| S7A, S9A | $y^1$ $v^1$/+ or Y; R71G10-QF2, QUAS-mtdT:3xHA/+; P{y[+t7.7] v[+t1.8]=TRiP.JF01355}attP2/+; OK107-Gal4/+ | UAS-Luciferase-RNAi (BL#31603) |
| S7B, S9B | $y^1$ $v^1$/+ or Y; R71G10-QF2, QUAS-mtdT:3xHA/+; P{y[+t7.7] v[+t1.8]=TRiP.JF01336}attP2/+; OK107-Gal4/+ | UAS-Mmp1-RNAi (BL#31489) |
| S7C, S9C | $y^1$ $v^1$/+ or Y; R71G10-QF2, QUAS-mtdT:3xHA/P{y[+t7.7] v[+t1.8]=TRiP.HMJ23143}attP40;; OK107-Gal4/+ | UAS-Mmp2-RNAi (BL#61309) |
| S7D, S9D | $y^1$ $v^1$/+ or Y; R71G10-QF2, QUAS-mtdT:3xHA/+; P{y[+t7.7] v[+t1.8]=TRiP.JF01355}attP2/Repo-Gal4, UAS-CD8:GFP | UAS-Luciferase-RNAi (BL#31603) |
| S7E, S9E | $y^1$ $v^1$/+ or Y; R71G10-QF2, QUAS-mtdT:3xHA/+; P{y[+t7.7] v[+t1.8]=TRiP.JF01336}attP2/Repo-Gal4, UAS-CD8:GFP | UAS-Mmp1-RNAi (BL#31489) |
| S7F, S9F | $y^1$ $v^1$/+ or Y; R71G10-QF2, QUAS-mtdT:3xHA/P{y[+t7.7] v[+t1.8]=TRiP.HMJ23143}attP40; Repo-Gal4, UAS-CD8:GFP/+ | UAS-Mmp2-RNAi (BL#61309) |

| | | |
|---|---|---|
| 4A | $y^1$ $v^1$/+ or Y; R71G10-QF2, QUAS-mtdT:3xHA/+; P{y[+t7.7] v[+t1.8]=TRiP.JF01336}attP2/Repo-Gal4, UAS-CD8:GFP | UAS-Mmp1-RNAi (BL#31489) |
| 4B | $y^1$ $v^1$/+ or Y; R71G10-QF2, QUAS-mtdT:3xHA/P{y[+t7.7] v[+t1.8]=TRiP.HMJ23143}attP40; Repo-Gal4, UAS-CD8:GFP/+ | UAS-Mmp2-RNAi (BL#61309) |
| 4C | $y^1$ $v^1$/+ or Y; R71G10-QF2, QUAS-mtdT:3xHA/P{y[+t7.7] v[+t1.8]=TRiP.HMJ23143}attP40; P{y[+t7.7] v[+t1.8]=TRiP.JF01336}attP2/Repo-Gal4, UAS-CD8:GFP | UAS-Mmp1-RNAi (BL#31489) **+** UAS-Mmp2-RNAi (BL#61309) |
| 4E | $y^1$ $v^1$ /+ or Y; R71G10-QF2, QUAS-mtdT:3xHA/+; P{y[+t7.7] v[+t1.8]=TRiP.JF01336}attP2/+; OK107-Gal4/+ | UAS-Mmp1-RNAi (BL#31489) |
| 4F | $y^1$ $v^1$/+ or Y; R71G10-QF2, QUAS-mtdT:3xHA/P{y[+t7.7] v[+t1.8]=TRiP.HMJ23143}attP40;; OK107-Gal4/+ | UAS-Mmp2-RNAi (BL#61309) |
| 4G | $y^1$ $v^1$/+ or Y; R71G10-QF2, QUAS-mtdT:3xHA/P{y[+t7.7] v[+t1.8]=TRiP.HMJ23143}attP40; P{y[+t7.7] v[+t1.8]=TRiP.JF01336}attP2/+; OK107-Gal4/+ | UAS-Mmp1-RNAi (BL#31489) **+** UAS-Mmp2-RNAi (BL#61309) |
| 4I | $y^1$ $v^1$/+ or Y; R71G10-QF2, QUAS-mtdT:3xHA/+; P{y[+t7.7] v[+t1.8]=TRiP.JF01336}attP2/Repo-Gal4, UAS-CD8:GFP; OK107-Gal4/+ | UAS-Mmp1-RNAi (BL#31489) |
| 4J | $y^1$ $v^1$/+ or Y; R71G10-QF2, QUAS-mtdT:3xHA/P{y[+t7.7] v[+t1.8]=TRiP.HMJ23143}attP40; Repo-Gal4 UAS-CD8:GFP/+; OK107-Gal4/+ | UAS-Mmp2-RNAi (BL#61309) |
| 4K | $y^1$ $v^1$/+ or Y; R71G10-QF2, QUAS-mtdT:3xHA/P{y[+t7.7] v[+t1.8]=TRiP.HMJ23143}attP40; P{y[+t7.7] v[+t1.8]=TRiP.JF01336}attP2/Repo-Gal4, UAS-CD8:GFP; OK107-Gal4/+ | UAS-Mmp1-RNAi (BL#31489) **+** UAS-Mmp2-RNAi (BL#61309) |
| S8A | $y^1$ $w^{118}$ /+ or Y; R71G10-QF2, QUAS-mtdT:3xHA/+; +/Alrm-Gal4 UAS-CD8::GFP | $y^1$ ,$w^{118}$ (BL#6598) |
| S8B | $y^1$ $v^1$/+ or Y; R71G10-QF2, QUAS-mtdT:3xHA/+; P{y[+t7.7] v[+t1.8]=TRiP.JF01336}attP2/Alrm-Gal4, UAS-CD8:GFP | UAS-Mmp1-RNAi (BL#31489) |
| S8C | $y^1$ $v^1$/+ or Y; R71G10-QF2, QUAS-mtdT:3xHA/P{y[+t7.7] v[+t1.8]=TRiP.HMJ23143}attP40; Alrm-Gal4, UAS-CD8:GFP/+ | UAS-Mmp2-RNAi (BL#61309) |

**Table 2.** Full *Drosophila* genotypes

*Immunohistochemistry and imaging*

*Drosophila* brains were dissected in cold ringer solution and placed on ice. Followed by fixation in 4% paraformaldehyde (PFA) solution for 20 min in room temperature (RT). Fixed brains were then washed with PB supplemented with 0.3% Triton X-(PBT) – 3 times, 20 min each. Next the brains were blocked for non-specific staining using 5% heat inactivated normal goat serum (NGS). Antibody staining was performed as follows: primary antibodies (4°C, overnight), PBT washes (X3 in RT, 20 min each), secondary antibodies (RT, 2h), PBT washes (X3 in RT, 20 min each), mounting in SlowFade (Invitrogen). Primary antibodies included mouse anti-FasII 1:25 (1D4; Developmental Studies Hybridoma Bank; DSHB), mouse anti-EcRB1 1:25 (AD4.4; DSHB), rat anti-HA 1:250 (Sigma Aldrich, 11867423001) and mouse anti-Mmp1 1:20 (mix of: 3A6B4, 3B8D12

319 and 5H7B11; DSHB). Secondary antibodies included Alexa fluor 647 goat anti-mouse
320 1:300 (A-21236; Invitrogen) and Alexa fluor 568 goat anti-rat 1:300 (A-21247; Invitrogen).
321 All brains were imaged on a Zeiss LSM980 confocal microscope. The images were
322 processed using ImageJ 2.14.0 (NIH).

323 *Generation of the mmp2 mutant allele*

324 The *mmp2* mutant allele named Δ54-120.C was generated by crossing a gRNA-line,
325 which harbors two distinct gRNA sequences both targeting the 5' CDS region common to
326 all 3 Mmp2 isoforms (cloned into pCFD4; BDSC #82521, WKO.3-C7), to a nanos-Cas9-
327 expressing fly. The recovered indel is a deletion of 67bp (54-120 in the CDS of isoform
328 C) – predicted to induce a premature stop codon (after 77 out of 606 amino acids in
329 isoform C). Unfortunately, this mutant (alongside many others) was lost on June 15$^{th}$ (see
330 acknowledgements).
331 The following primers were used to sequence the indel mutation:
332 F: GCATTCAATGCTGCCACAAA
333 R: CATTTCATCATCGACGTCGT

334 *Generation of MARCM clones*

335 γ-KC neuroblast clones were generated using the MARCM strategy (Lee & Luo,
336 1999). Newly hatched larvae (approximately 24h after egg laying) were heat-shocked for
337 1 hour in 37°C. Adult brains were dissected for further analysis.

338 *Quantification and statistical analysis*

339 Blind ranking of the pruning phenotypes for Fig. 3 and Fig. 4 were performed, for all
340 experiments, by two independent investigators who reviewed the Z-projections. Ranking
341 scores: 1 = WT-like phenotype, 2 = very mild pruning defect (PD), 3 = mild PD, 4 =
342 moderate PD, 5 = severe PD (Fig. S3A-E). The two sets of ranking were compared using
343 Wilcoxon signed rank test and found to be statistically insignificant (Fig. S3F-G).
344 A non-parametric statistical analysis was preformed to analyze the ranking (Fig. 3 and
345 Fig. 4): Kruskal Wallis H test followed by a post hoc Mann Whitney U test with FDR
346 correction.

347 *** = p value<0.001, ** = p value<0.01, * = p value<0.05, N.S = not significant. Specific p
348 values are indicated in the figure legends.
349

## Acknowledgements

We thank Andrea Page-McCaw (Vanderbilt University) for kindly sharing the Mmp1 dominant negative strain, and the Bloomington Drosophila Stock Center for reagents. Monoclonal antibodies were obtained from the Developmental Studies Hybridoma Bank developed under the auspices of the NICHD and maintained by the University of Iowa. We thank R. Rothkopf for assistance with statistics. This work was supported by European Research Council (ERC) advanced grant #101054886 "NeuRemodelBehavior," and by the ISF-NSFC joint research program (grant no. 2573/18). O.S is an incumbent of the Prof. Erwin Netter Professorial Chair of Cell Biology. On the night of June 15th 2025, our lab was directly hit by an Iranian missile and was completely destroyed. Unfortunately, this affects our abilily to provide reagents and limited the scope of our revisions.

## Author contributions

S.K. conceptualized the project, designed, performed and analyzed experiments, performed bioinformatic and statistical analyses, and wrote the manuscript. H.M. designed and performed experiments, interpreted results, and wrote the manuscript. N.M-K. designed experiments and assisted with bioinformatic analyses. O.S. led the project, designed experiments, interpreted results, wrote the manuscript, and procured funding.

## Declaration of interests

The authors declare that they have no conflict of interest.

A

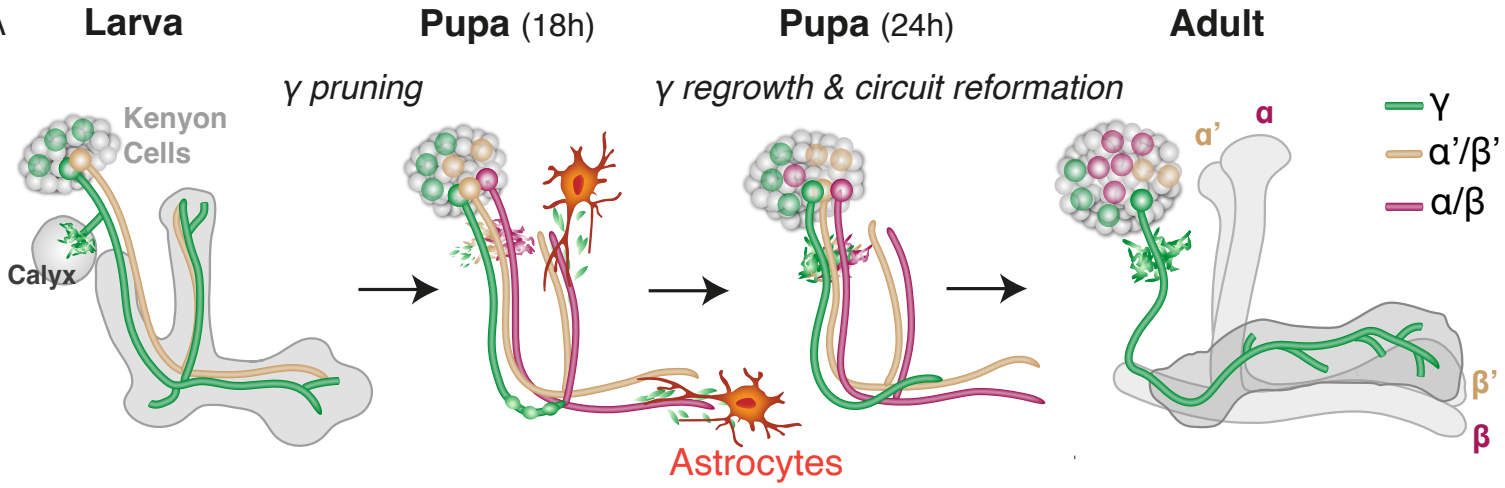


B

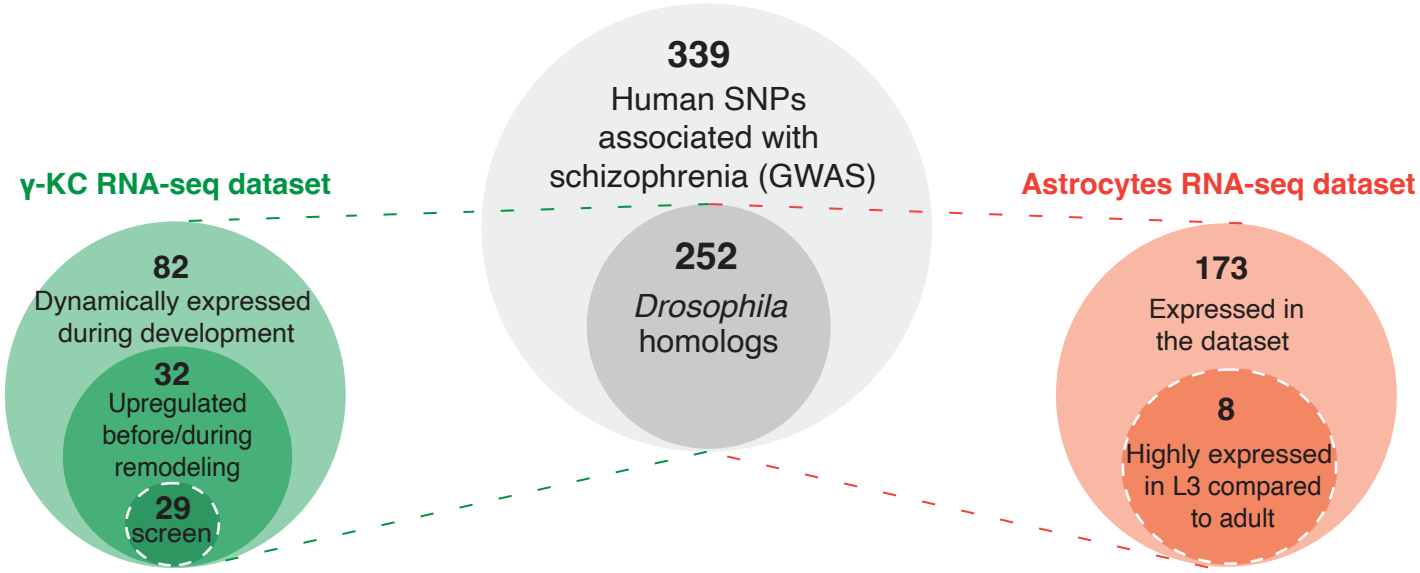


C Genes expressed in γ-KCs before/during remodeling

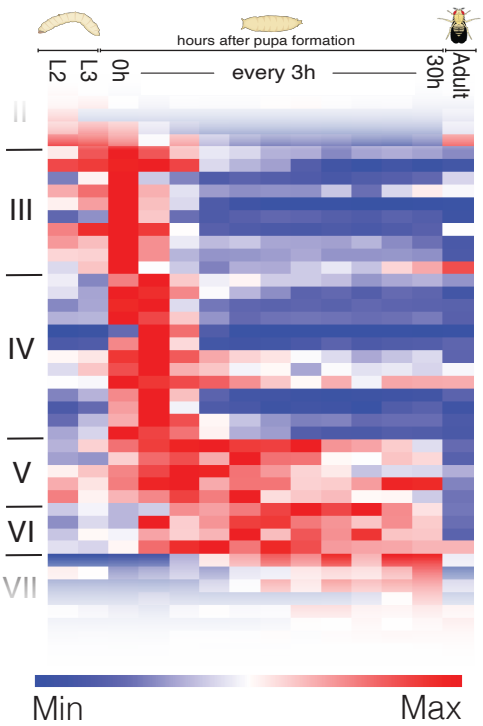


D Genes dynamically expressed in astrocytes

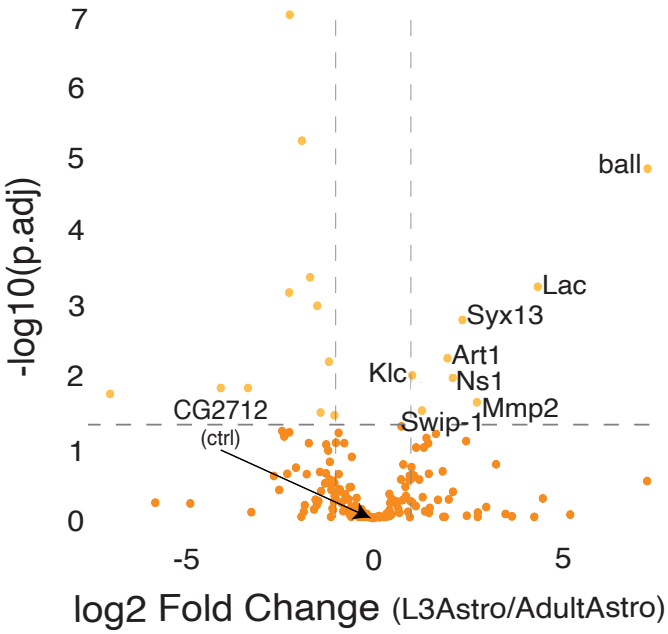

371 **Figure 1. *Drosophila* homologs of SCZ-associated genes are dynamically expressed in**
372 **developing mushroom body γ-KCs and in astrocytes.**

373 (A) Schematic representation of *Drosophila* MB development. During early pupal stages, only the
374 γ-KCs (green) prune their dendrites completely and their vertical and medial axonal branches up
375 to their branch-point. Subsequently, they reform dendrites in the calyx and regrow axons to form
376 the adult-specific medial lobe. Later-born α'/β'- and α/β-KCs, as well as astrocytes, are also
377 depicted.

378 (B) A schematic representation describing the logic of candidate selection for the loss-of-function
379 screen within KCs and glia. White dashed circles highlight the portion of genes that were
380 screened.

381 (C) A heatmap representing the expression of 32 genes (clusters III-VI) upregulated during/after
382 remodeling that were selected as candidates for screening (based on Alyagor et al., 2018). Each
383 row represents a gene, with red and blue indicating high and low relative expression, respectively.
384 The full heatmap of all dynamically expressed genes is available in Fig. S1.

385 (D) Volcano plot representing the comparison of gene expression between larval and adult
386 astrocytes (based on Marmor-Kollet et al., 2023). Annotated genes are expressed significantly
387 higher in L3 astrocytes compared to adult astrocytes. Each dot represents a gene, the x axis
388 represents the log2 fold change, the y axis represents the −log10 of the adjusted p value (p.adj).

389 For the full gene expression data and the candidate gene lists see Supplemental excel file 1.
390

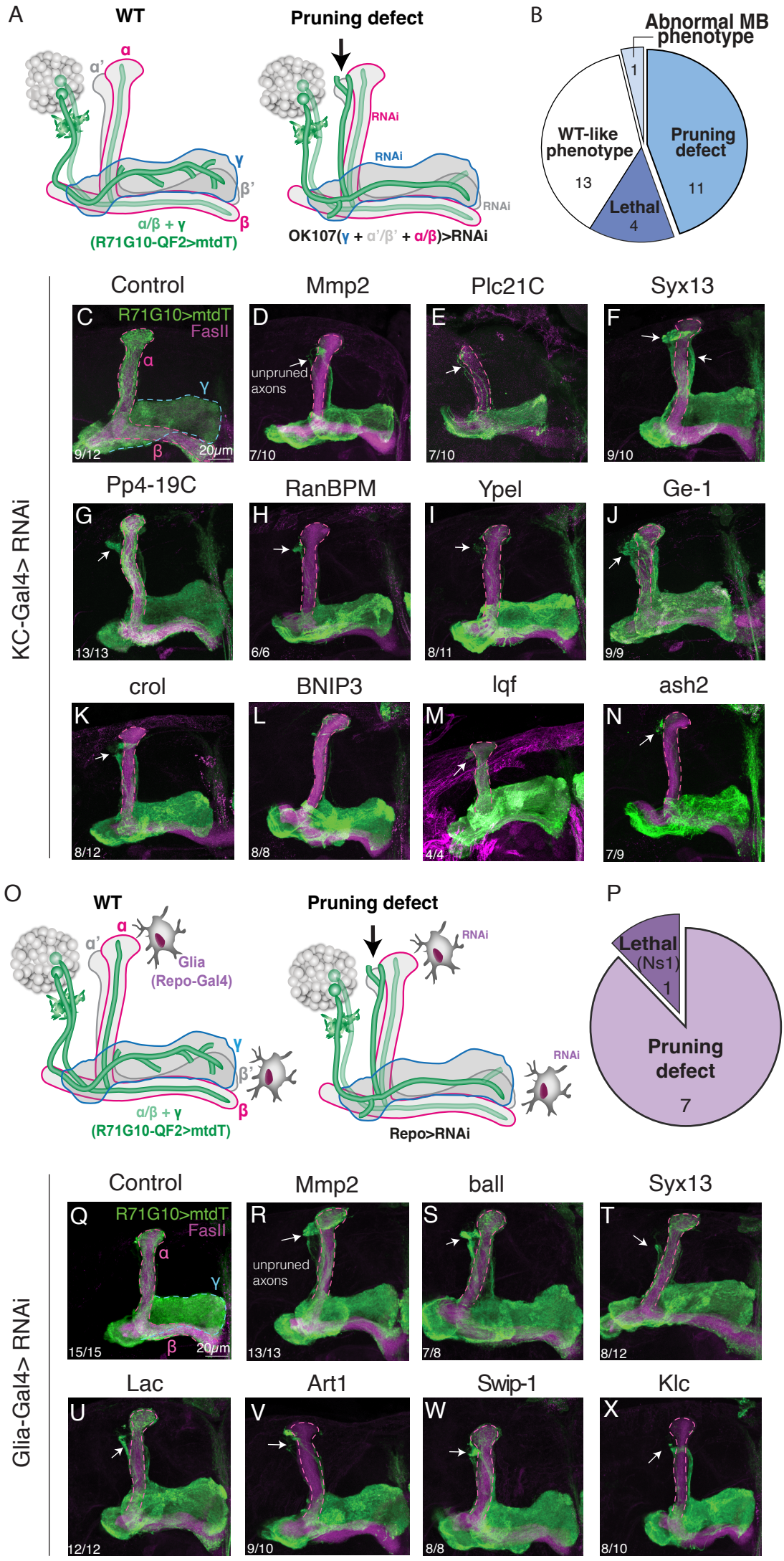
A
WT
Pruning defect
α
α'
γ
β'
β
α/β + γ
(R71G10-QF2>mtdT)
RNAi
RNAi
RNAi
OK107(γ + α'/β' + α/β)>RNAi
B
Abnormal MB phenotype
1
WT-like phenotype
13
Pruning defect
11
Lethal
4
KC-Gal4> RNAi
Control
Mmp2
Plc21C
Syx13
C
R71G10>mtdT
FasII
9/12
20μm
D
unpruned axons
7/10
E
7/10
F
9/10
Pp4-19C
RanBPM
Ypel
Ge-1
G
13/13
H
6/6
I
8/11
J
9/9
crol
BNIP3
lqf
ash2
K
8/12
L
8/8
M
4/4
N
7/9
O
WT
Glia
(Repo-Gal4)
α/β + γ
(R71G10-QF2>mtdT)
Pruning defect
RNAi
RNAi
Repo>RNAi
P
Lethal
(Ns1)
1
Pruning defect
7
Glia-Gal4> RNAi
Control
Mmp2
ball
Syx13
Q
R71G10>mtdT
FasII
15/15
20μm
R
unpruned axons
13/13
S
7/8
T
8/12
Lac
Art1
Swip-1
Klc
U
12/12
V
9/10
W
8/8
X
8/10

**Figure 2. *Drosophila* homologs of human SCZ-associated genes are required in neurons and glia for γ-axon pruning.**

(A) A schematic representation of the experimental design. RNAi transgenes targeting candidate genes were driven in KCs by the strong driver OK107-Gal4 (γ - blue outline, α/β - magenta outline, α'/β' - gray). The γ-axon pruning phenotype was examined in adult brains via the expression of myristoylated tandem Tomato (mtdT; green) driven by R71G10-QF2. Left: WT, all γ axons were pruned during pupal stages and regrew to form the adult specific medial γ lobe (blue outline). Note that R71G10-QF2 is also stochastically expressed in α/β neurons, which are additionally strongly positive to FasII (magenta outline). Right: pruning defect, some γ axons were not pruned - remanents of larval projections (arrow) are visible outside the highly fasciculated α axon bundle (magenta outline). Adapted with permission from Marmor-Kollet et al. 2023.

(B) Pie chart representing the overall KD screen results in KCs (see Supplemental excel file 1; for the abnormal MB phenotype see Fig. S2).

(C-N) Confocal z-projections of of adult MBs in which the indicated UAS-RNAi transgenes were expressed in all KCs using OK107-Gal4, while R71G10-QF2 drives the expression of mtdT (green) in γ-KCs and stochastically in α/β-KCs. The RNAi transgenes target the following genes: Matrix Metalloproteinase 2 (Mmp2; D), Phospholipase C at 21C (Plc21C; E), Syntaxin 13 (Syx13; F), Protein phosphatase 19C (Pp4-19C; G), Ran-binding protein M (RanBPM; H), Yippee-like (Ypel; I), Ge-1 (Ge-1; J), crooked legs (crol; K), BCL2 Interacting Protein 3 (BNIP3; L), liquid facets (lqf; M), absent, small, or homeotic discs 2 (ash2; N). Control is RNAi targeting Luciferase (C). FasII antibody (magenta) strongly labels α/β-KCs and weakly labels γ-KCs. The γ lobe is outlined in blue, and the α/β lobes are outlined in magenta.

(O) A schematic representation of the experimental design. RNAi transgenes targeting candidate genes were driven in all glia by Repo-Gal4 (gray cells). The γ axon pruning phenotype was examined in adult brains via the expression of mtdT (green) driven by R71G10-QF2.

(P) Pie chart representing the overall glial screen results (see Supplemental excel file 1).

(Q-X) Confocal z-projections of adult MBs in which the indicated UAS-RNAi transgenes were expressed in all glia cells using Repo-Gal4, while R71G10-QF2-drives the expression of mtdT (green) in γ-KCs and stochastically in α/β-KCs. The RNAi transgenes target the following genes: Matrix Metalloproteinase 2 (Mmp2; R), ballchen (ball; S), Syntaxin 13 (Syx13; T), Lachesin (Lac; U), Arginine methyltransferase 1 (Art1; V), Swiprosin-1 (Swip-1; W), Kinesin light chain (Klc; X). Control is RNAi targeting CG2712 (Q), which is expressed in near-zero levels (in both larval and adult astrocytes), as indicated by its location at the origin of the volcano plot (see Fig. 1D). FasII antibody (magenta) strongly labels α/β-axons and weakly labels γ-axons. The γ lobe is outlined in blue, and the α/β lobes are outlined in magenta.

Arrows indicate unpruned axons. Scale bar corresponds to 20μm. The number of MBs (each from an individual brain) showing the presented phenotype out of the total n for each genotype is indicated.

For all screened genes genotype and phenotype findings, see Supplemental excel file 1. Lines used in the screen appear in Table 1. Full genotypes appear in Table 2.

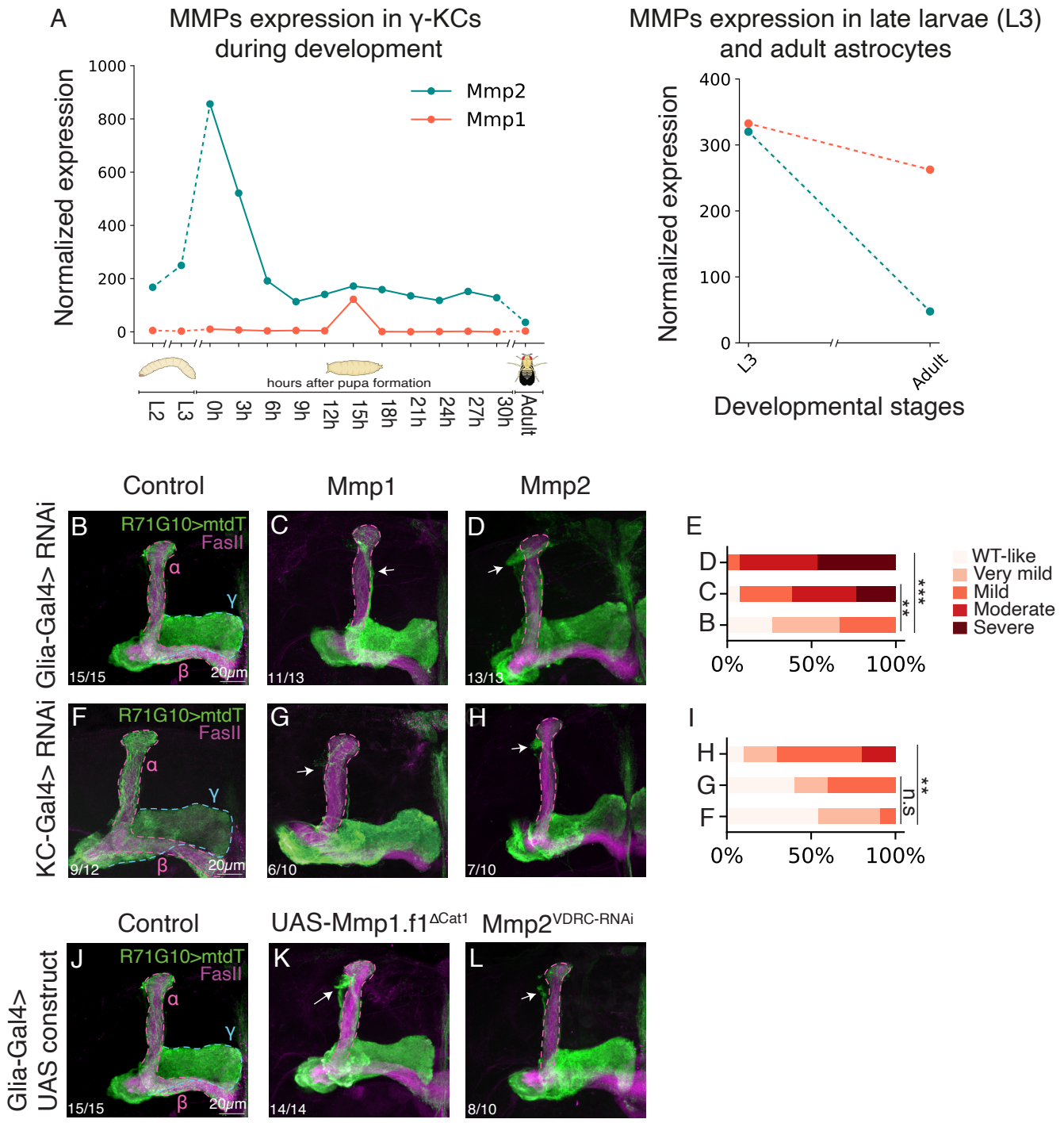
A
MMPs expression in γ-KCs during development
Normalized expression
Mmp2
Mmp1
hours after pupa formation
L2
L3
0h
3h
6h
9h
12h
15h
18h
21h
24h
27h
30h
Adult
MMPs expression in late larvae (L3) and adult astrocytes
Developmental stages
Control
Mmp1
Mmp2
Glia-Gal4> RNAi
KC-Gal4> RNAi
R71G10>mtdT
FasII
α
γ
β
20μm
15/15
11/13
13/13
9/12
6/10
7/10
WT-like
Very mild
Mild
Moderate
Severe
n.s
UAS-Mmp1.f1ΔCat1
Mmp2VDRC-RNAi
Glia-Gal4> UAS construct
14/14
8/10

433 **Figure 3. *Drosophila* MMPs are required in KCs and glia for γ-axon pruning.**
434 (A) Normalized gene expression of Mmp1 (orange) and Mmp2 (cyan) in developing γ-KCs (left;
435 based on Alyagor et al., 2018) and in larval/adult astrocytes (right; based on Marmor-Kollet et al.,
436 2023).
437 (B-D, F-H) Confocal z-projections of adult MBs in which γ-KCs are labeled by R71G10-QF2-driven
438 QUAS-mtdT (green). RNAi species targeting control genes (B, F), Mmp1 (C, G) or Mmp2 (D, H)
439 are expressed in all glia using Repo-Gal4 (B-D), or in all KCs using OK107-Gal4 (F-H).
440 Control in B is RNAi targeting CG2712 (see Fig. 1D), and in F is RNAi targeting Luciferase.
441 (E, I) Quantification of the pruning defect phenotypes, ranging from 1 (WT-like phenotype) to 5
442 (severe pruning defect). Genotypes are indicated with the letter of the corresponding image within
443 this figure. B vs. C p=0.001, B vs. D p=0.0001, F vs. G p=0.289, F vs. H p=0.009. *** = p<0.001,
444 * = p<0.05, n.s = not significant. For examples of quantification scores as well as ranking
445 comparison see Fig. S3.
446 (J-L) Confocal z-projections of adult MBs in which γ-KCs are labeled by R71G10-QF2-driven
447 QUAS-mtdT (green). Indicated UAS transgenes are driven by Repo-Gal4 Control in J is RNAi
448 targeting CG2712 (see Fig. 1D).
449 Arrows indicate unpruned axons. The γ lobe is outlines ib blue and the α/β lobes in magenta.
450 FasII antibody (magenta) strongly labels α/β-axons and weakly labels γ-axons. Scale bar
451 corresponds to 20μm.
452

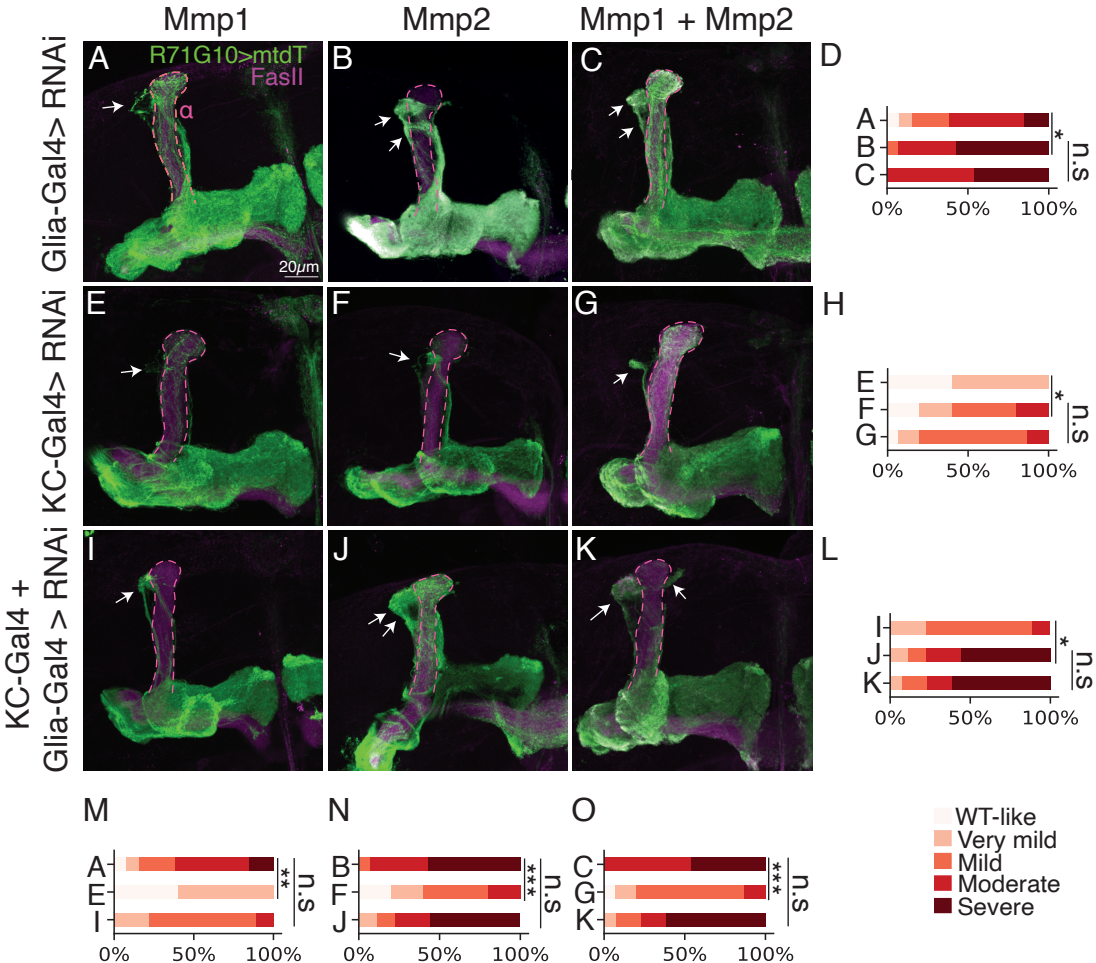
Mmp1
Mmp2
Mmp1 + Mmp2
Glia-Gal4> RNAi
KC-Gal4> RNAi
KC-Gal4 +
Glia-Gal4 > RNAi
R71G10>mtdT
FasII
α
20μm
A
B
C
D
E
F
G
H
I
J
K
L
M
N
O
0%
50%
100%
*
**
***
n.s
WT-like
Very mild
Mild
Moderate
Severe

453 **Figure 4. Analysis of combined MMP knockdown in both KCs and glia.**
454 (A-C, E-G, I-K) Confocal z-projections of adult MBs in which γ-KCs are labeled by R71G10-QF2-
455 driven QUAS-mtdT (green), and UAS-RNAi species targeting Mmp1 (A, E, I), Mmp2 (B, F J), or
456 both (C, G, K) are driven by Repo-Gal4 (A-C), OK107-Gal4 (E-G), or both simultaneously (I-K).
457 FasII antibody (magenta) strongly labels α/β-axons and weakly labels γ-axons. Arrows indicate
458 unpruned axons. The α-lobe is outlined in magenta.
459 (D, H, L-O) Quantification of the pruning defect phenotypes, ranging from 1 (WT-like phenotype)
460 to 5 (severe pruning defect). Genotypes are indicated with the letter of the corresponding image
461 within this figure. For quantification score examples and ranking comparison see Fig. S3. *** =
462 $p<0.001$, * = $p<0.05$, n.s = not significant.
463 A vs. B $p=0.023$, B vs. C $p=0.860$, E vs. F $p=0.046$, F vs. G $p=0.719$, I vs. J $p=0.023$, J vs. K
464 $p=0.943$, A vs. E $p=0.001$, A vs. I $p=0.092$, B vs. F $p=0.0009$, B vs. J $p=0.860$, C vs. G $p=0.0003$,
465 C vs. K $p=0.943$.
466
467
468

469 **References**


470 Alyagor, I., Berkun, V., Keren-Shaul, H., Marmor-Kollet, N., David, E., Mayseless, O., Issman-
471 Zecharya, N., Amit, I., & Schuldiner, O. (2018). Combining Developmental and
472 Perturbation-Seq Uncovers Transcriptional Modules Orchestrating Neuronal Remodeling.
473 *Dev Cell*, *47*(1), 38-52 e36. https://doi.org/10.1016/j.devcel.2018.09.013
474 Awasaki, T., Huang, Y., O'Connor, M. B., & Lee, T. (2011). Glia instruct developmental neuronal
475 remodeling through TGF-beta signaling. *Nat Neurosci*, *14*(7), 821-823.
476 https://doi.org/10.1038/nn.2833
477 Awasaki, T., & Ito, K. (2004). Engulfing action of glial cells is required for programmed axon
478 pruning during Drosophila metamorphosis. *Curr Biol*, *14*(8), 668-677.
479 https://doi.org/10.1016/j.cub.2004.04.001
480 Bornstein, B., Meltzer, H., Adler, R., Alyagor, I., Berkun, V., Cummings, G., Reh, F., Keren-
481 Shaul, H., David, E., Riemensperger, T., & Schuldiner, O. (2021). Transneuronal
482 Dpr12/DIP-delta interactions facilitate compartmentalized dopaminergic innervation of
483 Drosophila mushroom body axons. *EMBO J*, *40*(12), e105763.
484 https://doi.org/10.15252/embj.2020105763
485 Bornstein, B., Zahavi, E. E., Gelley, S., Zoosman, M., Yaniv, S. P., Fuchs, O., Porat, Z., Perlson,
486 E., & Schuldiner, O. (2015). Developmental Axon Pruning Requires Destabilization of Cell
487 Adhesion by JNK Signaling. *Neuron*, *88*(5), 926-940.
488 https://doi.org/10.1016/j.neuron.2015.10.023
489 Boulanger, A., Thinat, C., Züchner, S., Fradkin, L. G., Lortat-Jacob, H., & Dura, J.-M. (2021).
490 Axonal chemokine-like Orion induces astrocyte infiltration and engulfment during
491 mushroom body neuronal remodeling. *Nature Communications*, *12*(1), 1849.
492 https://doi.org/10.1038/s41467-021-22054-x
493 Brand, A. H., & Perrimon, N. (1993). Targeted gene expression as a means of altering cell
494 fates and generating dominant phenotypes. *Development*, *118*(2), 401-415.
495 https://doi.org/10.1242/dev.118.2.401
496 Brent, B. K., Thermenos, H. W., Keshavan, M. S., & Seidman, L. J. (2013). Gray matter
497 alterations in schizophrenia high-risk youth and early-onset schizophrenia: a review of
498 structural MRI findings. *Child Adolesc Psychiatr Clin N Am*, *22*(4), 689-714.
499 https://doi.org/10.1016/j.chc.2013.06.003
500 Broadie, K., Baumgartner, S., & Prokop, A. (2011). Extracellular matrix and its receptors in
501 Drosophila neural development. *Dev Neurobiol*, *71*(11), 1102-1130.
502 https://doi.org/10.1002/dneu.20935
503 Cox, T. R. (2021). The matrix in cancer. *Nature Reviews Cancer*, *21*(4), 217-238.
504 https://doi.org/10.1038/s41568-020-00329-7
505 Dear, M. L., Dani, N., Parkinson, W., Zhou, S., & Broadie, K. (2016). Two classes of matrix
506 metalloproteinases reciprocally regulate synaptogenesis. *Development*, *143*(1), 75-87.
507 https://doi.org/10.1242/dev.124461
508 Dickerson, F., Vaidya, D., Liu, Y., & Yolken, R. (2023). Levels of Matrix Metalloproteinase 9 Are
509 Elevated in Persons With Schizophrenia or Bipolar Disorder: The Role of Modifiable
510 Factors. *Biol Psychiatry Glob Open Sci*, *3*(4), 766-772.
511 https://doi.org/10.1016/j.bpsgos.2023.02.007
512 Feinberg, I. (1982). Schizophrenia: caused by a fault in programmed synaptic elimination
513 during adolescence? *J Psychiatr Res*, *17*(4), 319-334. https://doi.org/10.1016/0022-
514 3956(82)90038-3
515 Freeman, M. R. (2015). Drosophila Central Nervous System Glia. *Cold Spring Harb Perspect*
516 *Biol*, *7*(11). https://doi.org/10.1101/cshperspect.a020552

517 Furukubo-Tokunaga, K. (2009). Chapter 12 - Modeling schizophrenia in flies. In S. Akira (Ed.),
518 *Progress in Brain Research* (Vol. 179, pp. 107-115). Elsevier.
519 https://doi.org/https://doi.org/10.1016/S0079-6123(09)17912-8
520 Glasheen, B. M., Kabra, A. T., & Page-McCaw, A. (2009). Distinct functions for the catalytic
521 and hemopexin domains of a Drosophila matrix metalloproteinase. *Proc Natl Acad Sci U*
522 *S A*, *106*(8), 2659-2664. https://doi.org/10.1073/pnas.0804171106
523 Gore, S. V., James, E. J., Huang, L. C., Park, J. J., Berghella, A., Thompson, A. C., Cline, H.
524 T., & Aizenman, C. D. (2021). Role of matrix metalloproteinase-9 in neurodevelopmental
525 deficits and experience-dependent plasticity in Xenopus laevis. *Elife*, *10*.
526 https://doi.org/10.7554/eLife.62147
527 Hakim, Y., Yaniv, S. P., & Schuldiner, O. (2014). Astrocytes play a key role in Drosophila
528 mushroom body axon pruning. *PLoS One*, *9*(1), e86178.
529 https://doi.org/10.1371/journal.pone.0086178
530 Hamshere, M. L., Walters, J. T., Smith, R., Richards, A. L., Green, E., Grozeva, D., Jones, I.,
531 Forty, L., Jones, L., Gordon-Smith, K., Riley, B., O'Neill, F. A., Kendler, K. S., Sklar, P.,
532 Purcell, S., Kranz, J., Morris, D., Gill, M., Holmans, P., . . . O'Donovan, M. C. (2013).
533 Genome-wide significant associations in schizophrenia to ITIH3/4, CACNA1C and
534 SDCCAG8, and extensive replication of associations reported by the Schizophrenia PGC.
535 *Mol Psychiatry*, *18*(6), 708-712. https://doi.org/10.1038/mp.2012.67
536 Han, C., Song, Y., Xiao, H., Wang, D., Franc, N. C., Jan, L. Y., & Jan, Y. N. (2014). Epidermal
537 cells are the primary phagocytes in the fragmentation and clearance of degenerating
538 dendrites in Drosophila. *Neuron*, *81*(3), 544-560.
539 https://doi.org/10.1016/j.neuron.2013.11.021
540 Harmansa, S., Erlich, A., Eloy, C., Zurlo, G., & Lecuit, T. (2023). Growth anisotropy of the
541 extracellular matrix shapes a developing organ. *Nature Communications*, *14*(1), 1220.
542 https://doi.org/10.1038/s41467-023-36739-y
543 Heisenberg, M. (1998). What do the mushroom bodies do for the insect brain? an introduction.
544 *Learn Mem*, *5*(1-2), 1-10.
545 Hidalgo, S., Campusano, J. M., & Hodge, J. J. L. (2021). The Drosophila ortholog of the
546 schizophrenia-associated CACNA1A and CACNA1B voltage-gated calcium channels
547 regulate memory, sleep and circadian rhythms. *Neurobiol Dis*, *155*, 105394.
548 https://doi.org/10.1016/j.nbd.2021.105394
549 Hoffman, R. E., & Dobscha, S. K. (1989). Cortical pruning and the development of
550 schizophrenia: a computer model. *Schizophr Bull*, *15*(3), 477-490.
551 https://doi.org/10.1093/schbul/15.3.477
552 Huntley, G. W. (2012). Synaptic circuit remodelling by matrix metalloproteinases in health and
553 disease. *Nat Rev Neurosci*, *13*(11), 743-757. https://doi.org/10.1038/nrn3320
554 Huttenlocher, P. R., & Dabholkar, A. S. (1997). Regional differences in synaptogenesis in
555 human cerebral cortex. *J Comp Neurol*, *387*(2), 167-178.
556 https://doi.org/10.1002/(sici)1096-9861(19971020)387:2<167::aid-cne1>3.0.co;2-z
557 Keshavan, M., Lizano, P., & Prasad, K. (2020). The synaptic pruning hypothesis of
558 schizophrenia: promises and challenges. *World Psychiatry*, *19*(1), 110-111.
559 https://doi.org/https://doi.org/10.1002/wps.20725
560 Keshavan, M. S., Anderson, S., & Pettergrew, J. W. (1994). Is Schizophrenia due to excessive
561 synaptic pruning in the prefrontal cortex? The Feinberg hypothesis revisited. *Journal of*
562 *Psychiatric Research*, *28*(3), 239-265. https://doi.org/https://doi.org/10.1016/0022-
563 3956(94)90009-4
564 Kudo, N., Yamamori, H., Ishima, T., Nemoto, K., Yasuda, Y., Fujimoto, M., Azechi, H., Niitsu,
565 T., Numata, S., Ikeda, M., Iyo, M., Ohmori, T., Fukunaga, M., Watanabe, Y., Hashimoto,
566 K., & Hashimoto, R. (2020). Plasma levels of matrix metalloproteinase-9 (MMP-9) are

associated with cognitive performance in patients with schizophrenia. *Neuropsychopharmacol Rep*, *40*(2), 150-156. https://doi.org/10.1002/npr2.12098

Kuo, C. T., Jan, L. Y., & Jan, Y. N. (2005). Dendrite-specific remodeling of Drosophila sensory neurons requires matrix metalloproteases, ubiquitin-proteasome, and ecdysone signaling. *Proceedings of the National Academy of Sciences*, *102*(42), 15230-15235. https://doi.org/doi:10.1073/pnas.0507393102

LaFever, K. S., Wang, X., Page-McCaw, P., Bhave, G., & Page-McCaw, A. (2017). Both Drosophila matrix metalloproteinases have released and membrane-tethered forms but have different substrates. *Scientific Reports*, *7*(1), 44560. https://doi.org/10.1038/srep44560

Laricchiuta, D., Papi, M., Decandia, D., Panuccio, A., Cutuli, D., Peciccia, M., Mazzeschi, C., & Petrosini, L. (2024). The role of glial cells in mental illness: a systematic review on astroglia and microglia as potential players in schizophrenia and its cognitive and emotional aspects. *Front Cell Neurosci*, *18*, 1358450. https://doi.org/10.3389/fncel.2024.1358450

Lee, T., Lee, A., & Luo, L. (1999). Development of the Drosophila mushroom bodies: sequential generation of three distinct types of neurons from a neuroblast. *Development*, *126*(18), 4065-4076. https://www.ncbi.nlm.nih.gov/pubmed/10457015

Lee, T., & Luo, L. (1999). Mosaic analysis with a repressible cell marker for studies of gene function in neuronal morphogenesis. *Neuron*, *22*(3), 451-461. https://doi.org/10.1016/s0896-6273(00)80701-1

Lepeta, K., Purzycka, K. J., Pachulska-Wieczorek, K., Mitjans, M., Begemann, M., Vafadari, B., Bijata, K., Adamiak, R. W., Ehrenreich, H., Dziembowska, M., & Kaczmarek, L. (2017). A normal genetic variation modulates synaptic MMP-9 protein levels and the severity of schizophrenia symptoms. *EMBO Mol Med*, *9*(8), 1100-1116. https://doi.org/10.15252/emmm.201707723

Lessing, D., & Bonini, N. M. (2009). Maintaining the brain: insight into human neurodegeneration from Drosophila melanogaster mutants. *Nat Rev Genet*, *10*(6), 359-370. https://doi.org/10.1038/nrg2563

Li, T., Shi, W., Ho, M. S., & Zhang, Y. Q. (2024). A Pvr–AP-1–Mmp1 signaling pathway is activated in astrocytes upon traumatic brain injury. In: eLife Sciences Publications, Ltd.

Llano, E., Adam, G., Pendás, A. M., Quesada, V. c., Sánchez, L. M., Santamaría, I., Noselli, S., & López-Otín, C. (2002). Structural and Enzymatic Characterization of Drosophila Dm2-MMP, a Membrane-bound Matrix Metalloproteinase with Tissue-specific Expression*. *Journal of Biological Chemistry*, *277*(26), 23321-23329. https://doi.org/https://doi.org/10.1074/jbc.M200121200

Luo, L., & O'Leary, D. D. (2005). Axon retraction and degeneration in development and disease. *Annu Rev Neurosci*, *28*, 127-156. https://doi.org/10.1146/annurev.neuro.28.061604.135632

Lyne, R., Bazaga, A., Butano, D., Contrino, S., Heimbach, J., Hu, F., Kalderimis, A., Lyne, M., Reierskog, K., Stepan, R., Sullivan, J., Wise, A., Yehudi, Y., & Micklem, G. (2022). HumanMine: advanced data searching, analysis and cross-species comparison. *Database*, *2022*, baac054. https://doi.org/10.1093/database/baac054

Marmor-Kollet, N., Berkun, V., Cummings, G., Keren-Shaul, H., David, E., Addadi, Y., & Schuldiner, O. (2023). Actin-dependent astrocytic infiltration is a key step for axon defasciculation during remodeling. *Cell Reports*, *42*(2), 112117. https://doi.org/https://doi.org/10.1016/j.celrep.2023.112117

McCutcheon, R. A., Reis Marques, T., & Howes, O. D. (2020). Schizophrenia-An Overview. *JAMA Psychiatry*, *77*(2), 201-210. https://doi.org/10.1001/jamapsychiatry.2019.3360

Meltzer, H., Marom, E., Alyagor, I., Mayseless, O., Berkun, V., Segal-Gilboa, N., Unger, T., Luginbuhl, D., & Schuldiner, O. (2019). Tissue-specific (ts)CRISPR as an efficient strategy

for in vivo screening in Drosophila. *Nat Commun*, *10*(1), 2113. https://doi.org/10.1038/s41467-019-10140-0

Notter, T. (2021). Astrocytes in schizophrenia. *Brain Neurosci Adv*, *5*, 23982128211009148. https://doi.org/10.1177/23982128211009148

Omlor, W., Rabe, F., Fuchs, S., Surbeck, W., Cecere, G., Huang, G. Y., Homan, S., Kallen, N., Georgiadis, F., Spiller, T., Seifritz, E., Weickert, T., Bruggemann, J., Weickert, C., Potkin, S., Hashimoto, R., Sim, K., Rootes-Murdy, K., Quide, Y., . . . Homan, P. (2025). Estimating Multimodal Structural Brain Variability in Schizophrenia Spectrum Disorders: A Worldwide ENIGMA Study. *Am J Psychiatry*, *182*(4), 373-388. https://doi.org/10.1176/appi.ajp.20230806

Overall, C. M., & López-Otín, C. (2002). Strategies for MMP inhibition in cancer: innovations for the post-trial era. *Nat Rev Cancer*, *2*(9), 657-672. https://doi.org/10.1038/nrc884

Page-McCaw, A., Ewald, A. J., & Werb, Z. (2007). Matrix metalloproteinases and the regulation of tissue remodelling. *Nat Rev Mol Cell Biol*, *8*(3), 221-233. https://doi.org/10.1038/nrm2125

Penzes, P., Cahill, M. E., Jones, K. A., VanLeeuwen, J.-E., & Woolfrey, K. M. (2011). Dendritic spine pathology in neuropsychiatric disorders. *Nature Neuroscience*, *14*(3), 285-293. https://doi.org/10.1038/nn.2741

Peter R, H. (1979). Synaptic density in human frontal cortex — Developmental changes and effects of aging. *Brain Research*, *163*(2), 195-205. https://doi.org/https://doi.org/10.1016/0006-8993(79)90349-4

Pijet, B., Stefaniuk, M., & Kaczmarek, L. (2019). MMP-9 Contributes to Dendritic Spine Remodeling Following Traumatic Brain Injury. *Neural Plast*, *2019*, 3259295. https://doi.org/10.1155/2019/3259295

Purice, M. D., Ray, A., Münzel, E. J., Pope, B. J., Park, D. J., Speese, S. D., & Logan, M. A. (2017). A novel Drosophila injury model reveals severed axons are cleared through a Draper/MMP-1 signaling cascade. *Elife*, *6*. https://doi.org/10.7554/eLife.23611

Riabinina, O., & Potter, C. J. (2016). The Q-System: A Versatile Expression System for Drosophila. *Methods Mol Biol*, *1478*, 53-78. https://doi.org/10.1007/978-1-4939-6371-3_3

Sawamura, N., Ando, T., Maruyama, Y., Fujimuro, M., Mochizuki, H., Honjo, K., Shimoda, M., Toda, H., Sawamura-Yamamoto, T., Makuch, L. A., Hayashi, A., Ishizuka, K., Cascella, N. G., Kamiya, A., Ishida, N., Tomoda, T., Hai, T., Furukubo-Tokunaga, K., & Sawa, A. (2008). Nuclear DISC1 regulates CRE-mediated gene transcription and sleep homeostasis in the fruit fly. *Mol Psychiatry*, *13*(12), 1138-1148, 1069. https://doi.org/10.1038/mp.2008.101

Schoretsanitis, G., de Filippis, R., Ntogka, M., Leucht, S., Correll, C. U., & Kane, J. M. (2021). Matrix Metalloproteinase 9 Blood Alterations in Patients With Schizophrenia Spectrum Disorders: A Systematic Review and Meta-Analysis. *Schizophr Bull*, *47*(4), 986-996. https://doi.org/10.1093/schbul/sbab001

Schuldiner, O., & Yaron, A. (2015). Mechanisms of developmental neurite pruning. *Cell Mol Life Sci*, *72*(1), 101-119. https://doi.org/10.1007/s00018-014-1729-6

Scott-Hewitt, N., Huang, Y., & Stevens, B. (2023). Convergent mechanisms of microglia-mediated synaptic dysfunction contribute to diverse neuropathological conditions. *Annals of the New York Academy of Sciences*, *1525*(1), 5-27. https://doi.org/https://doi.org/10.1111/nyas.15010

Seitz-Holland, J., Seethaler, M., Makris, N., Rushmore, J., Cho, K. K., Rizzoni, E., Vangel, M., Sahin, O. S., Heller, C., Pasternak, O., Szczepankiewicz, F., Westin, C. F., Lošák, J., Ustohal, L., Tomandl, J., Vojtíšek, L., Kudlička, P., Jáni, M., Woo, T. W., . . . Kubicki, M. (2022). The association of matrix metalloproteinase 9 (MMP9) with hippocampal volume in schizophrenia: a preliminary MRI study. *Neuropsychopharmacology*, *47*(2), 524-530. https://doi.org/10.1038/s41386-021-00997-5

668 Sekar, A., Bialas, A. R., de Rivera, H., Davis, A., Hammond, T. R., Kamitaki, N., Tooley, K.,
669 Presumey, J., Baum, M., Van Doren, V., Genovese, G., Rose, S. A., Handsaker, R. E.,
670 Schizophrenia Working Group of the Psychiatric Genomics, C., Daly, M. J., Carroll, M. C.,
671 Stevens, B., & McCarroll, S. A. (2016). Schizophrenia risk from complex variation of
672 complement component 4. *Nature*, *530*(7589), 177-183.
673 https://doi.org/10.1038/nature16549
674 Sellgren, C. M., Gracias, J., Watmuff, B., Biag, J. D., Thanos, J. M., Whittredge, P. B., Fu, T.,
675 Worringer, K., Brown, H. E., Wang, J., Kaykas, A., Karmacharya, R., Goold, C. P.,
676 Sheridan, S. D., & Perlis, R. H. (2019). Increased synapse elimination by microglia in
677 schizophrenia patient-derived models of synaptic pruning. *Nat Neurosci*, *22*(3), 374-385.
678 https://doi.org/10.1038/s41593-018-0334-7
679 Sreesada, P., Vandana, Krishnan, B., Amrutha, R., Chavan, Y., Alfia, H., Jyothis, A., Venugopal,
680 P., Aradhya, R., Suravajhala, P., & Nair, B. G. (2025). Matrix metalloproteinases: Master
681 regulators of tissue morphogenesis. *Gene*, *933*, 148990.
682 https://doi.org/10.1016/j.gene.2024.148990
683 Suzuki, M., Nohara, S., Hagino, H., Kurokawa, K., Yotsutsuji, T., Kawasaki, Y., Takahashi, T.,
684 Matsui, M., Watanabe, N., Seto, H., & Kurachi, M. (2002). Regional changes in brain gray
685 and white matter in patients with schizophrenia demonstrated with voxel-based analysis
686 of MRI. *Schizophrenia Research*, *55*(1), 41-54.
687 https://doi.org/https://doi.org/10.1016/S0920-9964(01)00224-9
688 Szklarczyk, A., Lapinska, J., Rylski, M., McKay, R. D., & Kaczmarek, L. (2002). Matrix
689 metalloproteinase-9 undergoes expression and activation during dendritic remodeling in
690 adult hippocampus. *J Neurosci*, *22*(3), 920-930. https://doi.org/10.1523/jneurosci.22-03-
691 00920.2002
692 Tasdemir-Yilmaz, O. E., & Freeman, M. R. (2014). Astrocytes engage unique molecular
693 programs to engulf pruned neuronal debris from distinct subsets of neurons. *Genes Dev*,
694 *28*(1), 20-33. https://doi.org/10.1101/gad.229518.113
695 Truman, J. W. (1990). Metamorphosis of the central nervous system of Drosophila. *J*
696 *Neurobiol*, *21*(7), 1072-1084. https://doi.org/10.1002/neu.480210711
697 van Alphen, B., & van Swinderen, B. (2013). Drosophila strategies to study psychiatric
698 disorders. *Brain Res Bull*, *92*, 1-11. https://doi.org/10.1016/j.brainresbull.2011.09.007
699 Watts, R. J., Schuldiner, O., Perrino, J., Larsen, C., & Luo, L. (2004). Glia engulf degenerating
700 axons during developmental axon pruning. *Curr Biol*, *14*(8), 678-684.
701 https://doi.org/10.1016/j.cub.2004.03.035
702 Wu, Y., Yao, Y. G., & Luo, X. J. (2017). SZDB: A Database for Schizophrenia Genetic Research.
703 *Schizophr Bull*, *43*(2), 459-471. https://doi.org/10.1093/schbul/sbw102
704 Yaniv, S. P., & Schuldiner, O. (2016). A fly's view of neuronal remodeling. *Wiley Interdiscip Rev*
705 *Dev Biol*, *5*(5), 618-635. https://doi.org/10.1002/wdev.241
706 Yasunaga, K., Kanamori, T., Morikawa, R., Suzuki, E., & Emoto, K. (2010). Dendrite reshaping
707 of adult Drosophila sensory neurons requires matrix metalloproteinase-mediated
708 modification of the basement membranes. *Dev Cell*, *18*(4), 621-632.
709 https://doi.org/10.1016/j.devcel.2010.02.010
710 Yu, Q., & Stamenkovic, I. (2000). Cell surface-localized matrix metalloproteinase-9
711 proteolytically activates TGF-beta and promotes tumor invasion and angiogenesis. *Genes*
712 *Dev*, *14*(2), 163-176.
713 Yu, X. M., Gutman, I., Mosca, T. J., Iram, T., Ozkan, E., Garcia, K. C., Luo, L., & Schuldiner,
714 O. (2013). Plum, an immunoglobulin superfamily protein, regulates axon pruning by
715 facilitating TGF-beta signaling. *Neuron*, *78*(3), 456-468.
716 https://doi.org/10.1016/j.neuron.2013.03.004
717 Zheng, X., Wang, J., Haerry, T. E., Wu, A. Y., Martin, J., O'Connor, M. B., Lee, C. H., & Lee, T.
718 (2003). TGF-beta signaling activates steroid hormone receptor expression during

neuronal remodeling in the Drosophila brain. *Cell*, *112*(3), 303-315. https://doi.org/10.1016/s0092-8674(03)00072-2

Zikidi, K., Gajwani, R., Gross, J., Gumley, A. I., Lawrie, S. M., Schwannauer, M., Schultze-Lutter, F., Fracasso, A., & Uhlhaas, P. J. (2020). Grey-matter abnormalities in clinical high-risk participants for psychosis. *Schizophr Res*, *226*, 120-128. https://doi.org/10.1016/j.schres.2019.08.034